J. Am. Soc. Mass Spectrom. (2011) 22:408–417
DOI: 10.1007/s13361-010-0052-1

RESEARCH ARTICLE

# Protein–Protein Binding Affinities in Solution Determined by Electrospray Mass Spectrometry

Jiangjiang Liu, Lars Konermann

Department of Chemistry, The University of Western Ontario, N6A 5B7 London, Ontario, Canada

**Abstract**

Electrospray ionization (ESI) allows the transfer of multi-protein complexes into the gas phase, thereby providing a simple approach for monitoring the stoichiometry of these noncovalent assemblies by mass spectrometry (MS). It remains unclear, however, whether the measured ion abundance ratios of free and bound species are suitable for determining solution-phase binding affinities ($K_d$ values). Many types of mass spectrometers employ rf-only quadrupoles as ion guides. This work demonstrates that the settings used for these devices are a key factor for ensuring uniform transmission behavior, which is a prerequisite for meaningful affinity measurements. Using bovine β-lactoglobulin and hemoglobin as model systems, it is demonstrated that under carefully adjusted conditions the "direct" ESI-MS approach is capable of providing $K_d$ values that are in good agreement with previously published solution-phase data. Of the several ion sources tested, a regular ESI emitter operated with pressure-driven flow at 1 μL $min^{-1}$ provided the most favorable results. Potential problems in these experiments include conformationally-induced differences in ionization efficiencies, inadvertent collision-induced dissociation, and ESI-induced clustering artifacts. A number of simple tests can be conducted to assess whether or not these factors are prevalent under the conditions used. In addition, the fidelity of the method can be scrutinized by performing measurements over a wide concentration range. Overall, this work supports the viability of the direct ESI-MS approach for determining binding affinities of protein–protein complexes in solution.

**Key words:** Protein complex, Noncovalent interactions, Dissociation constant, Electrospray ionization, Biological mass spectrometry

## Introduction

Many proteins form noncovalent complexes with ligands such as metal ions, cofactors, or other proteins. Multi-protein complexes are of particular interest because they play a central role in numerous biological processes. The architecture of these supramolecular assemblies ranges from simple dimers all the way to systems that encompass dozens of subunits [1]. Various experimental methods have been applied for studying protein–protein interactions. These include optical and calorimetric assays [2], nuclear magnetic resonance spectroscopy [3], surface plasmon resonance [4], micro-array chips [5], yeast two-hybrid screens [6], and analytical ultracentrifugation (AUC) [7]. Mass spectrometry (MS) offers a number of complementary avenues for characterizing protein–protein interactions [8]. Hydrogen/deuterium exchange MS monitors changes in structure and dynamics upon binding [9–11]. Similarly, alterations in solvent accessibility can be probed by covalent labeling in solution, followed by a MS-based readout [12, 13]. Affinity purification/MS has proven to be highly effective as well [14, 15].

Conceptually, the most straightforward technique for monitoring noncovalent complexes by MS is the "direct" approach. This method involves the transfer of intact solution phase assemblies into the gas phase by electrospray (ESI) or related ionization processes, followed by detection in a suitable mass analyzer [16–20]. Attractive features of this strategy include its speed, sensitivity, and selectivity.

*Correspondence to:* Lars Konermann; *e-mail:* konerman@uwo.ca

Received: 27 October 2010
Revised: 10 December 2010
Accepted: 25 November 2010
Published online: 1 February 2011

Numerous laboratories have used the direct ESI-MS approach for characterizing protein–protein complexes [16–20], as well as other noncovalent assemblies [21–25].

One question that remains somewhat unclear is to what extent the direct ESI-MS approach is suitable for determining solution phase binding affinities. This issue has been explored in considerable detail for protein–small molecule complexes [26–29]. In comparison, affinity measurements for protein–protein interactions have received less attention. We will consider the simple example of a homodimer $D$ that is in equilibrium with its monomeric form $M$ in solution according to

$$D \rightleftharpoons 2\,M \tag{1}$$

The binding affinity of the complex is reflected in the dissociation constant

$$K_d = \frac{[M]^2}{[D]} \tag{2}$$

where $[M]$ and $[D]$ denote the equilibrium concentrations of monomer and dimer, respectively. Assuming that the concentration ratio

$$R_{sol} = \frac{[D]}{[M]} \tag{3}$$

in solution is known, the dissociation constant can be calculated as

$$K_d = [P]_0 \, \frac{1}{R_{sol}(2R_{sol} + 1)} \tag{4}$$

where $[P]_0 = [M] + 2[D]$ is the total protein concentration, expressed on a monomer basis. It is important to recognize that ESI-MS does *not* directly report the value of $R_{sol}$. Instead, these experiments provide the ion abundance ratio $R_{ESI-MS}$, which is given by

$$R_{ESI-MS} = \frac{I_D}{I_M} \tag{5}$$

where $I_D$ and $I_M$ are the integrated signal intensities of dimeric and monomeric ions. The relationship between signal intensity and solution-phase concentration is given by

$$I_D = \gamma D\,[D] \tag{6a}$$

$$I_M = \gamma_M [M] \tag{6b}$$

The response factors $\gamma$ reflect the extent to which $M$ and $D$ species in bulk solution are converted to measurable ESI-MS signals [30]. The magnitude of $\gamma$ depends on several factors, including how efficiently the species are (1) transformed into gaseous ions, (2) transmitted from the ESI source into the vacuum and through the mass spectrometer, and (3) converted into electronic signals at the detector. Knowledge of $\gamma_M/\gamma_D$ is vital for the use of ESI-MS as a tool for binding affinity measurements on the basis of Equation 4, since

$$R_{sol} = \frac{\gamma_M}{\gamma_D} R_{ESI-MS} \tag{7}$$

Methods for determining ESI-MS response factors have been proposed [30, 31], but those approaches are not straightforward and their general applicability remains unclear. Hence, it is common to postulate that $\gamma_M/\gamma_D \approx 1$ [32].

In addition to discussing $K_d$ values, a useful quantity that expresses the extent of protein interactions in solution is the fraction bound, $f_{sol}$, defined as

$$f_{sol} = 2\frac{[D]}{[P]_0} \tag{8}$$

ESI-MS provides a related value, $f_{ESI-MS}$, which is based on ion intensities according to

$$f_{ESI-MS} = 2\frac{I_D}{I_M + 2I_D} \tag{9}$$

Analogous to the discussion above, it is seen that $f_{sol} = f_{ESI-MS}$ only if $\gamma_M = \gamma_D$.

The assumption that free and bound solution-phase species have the same $\gamma$ value is relatively unproblematic in the case of small molecule binding to a large receptor, where the free and bound forms generate ions that cover a very similar *m/z* range [23, 27, 28]. For protein complexes, however, the situation is not as simple. The formation of protein–protein interactions may be associated with changes in physicochemical properties that can affect the response factors [33, 34]. The most obvious of these parameters are size and molecular weight. Smaller species tend to produce higher signal intensities [35]. Mass (or *m/z*) discrimination effects of this type can be caused by various factors, including insufficient collisional focusing during ion transfer [17, 18, 36, 37].

Discrimination phenomena can also be related to the ESI mechanism. Formation of a protein complex can change the percentage of solvent-exposed hydrophobic residues, for example when monomers undergo a folding transition upon binding. Differences between $\gamma_M$ and $\gamma_D$ would be expected in such a case because hydrophobicity is closely linked to the ESI ionization efficiency of proteins [38] as well as other analytes [39, 40]. Also, solution phase equilibria may shift due to acidification caused by redox reactions in the ESI capillary [27, 41, 42], or as the result of concentration changes in the shrinking ESI droplets [43]. Luckily, these

equilibrium shifts tend to be small under typical operating conditions [35, 44]. Of greater concern is the possibility that nonspecific complexes can be formed from ESI droplets that contain two or more protein molecules. ESI-induced artifacts of this type can give rise to false-positive results, i.e., the observation of gas-phase complexes that did not exist in solution [17, 32, 35, 45]. Conversely, protein complexes may get disrupted during or after ESI, for example by collision-induced dissociation (CID) [19, 35, 46–49].

Whereas regular ESI employs flow rates in the μL $min^{-1}$ range, nanoESI sources are operated in the nL $min^{-1}$ regime [50, 51]. It is often implied that nanoESI methods provide a better reflection of solution-phase binding equilibria due to the purported greater "softness" of the ionization process [17]. Nano-ESI-MS certainly offers some advantages due to its low sample consumption. The notion that it better reflects solution-phase binding equilibria, however, is not undisputed [26, 46].

The preceding considerations show that ESI-MS may provide a distorted view of solution phase binding equilibria in certain cases. To examine the applicability of the direct ESI-MS approach for protein–protein affinity measurements, the current work focuses on two systems, β-lactoglobulin (BLG) [32, 52, 53] and hemoglobin (Hb) [54–56]. We test the effects of different ion sources. The extent to which differential protein ionization efficiencies, inadvertent fragmentation, and artifactual clustering affect the measured data are explored. Dramatically skewed results are obtained when employing improper ion transfer settings. Nonetheless, we find that under carefully controlled conditions the mass spectra reflect the protein binding behavior in solution remarkably well.

## Experimental

### *Materials*

Bovine BLG (monomer mass 18281 Da, PDB code 1BEB) was purchased from Sigma (St. Louis, MO, USA). Protein purity was confirmed by SDS gel electrophoresis. Hb (PDB code 2QSS) was isolated from fresh cow blood in its oxygenated (ferro) form following established procedures [56]. The masses of the Hb α and β subunits (including heme, excluding oxygen) are 15,669 and 16,570 Da, respectively. Prior to ESI-MS, the proteins were extensively dialyzed against 10 mM aqueous ammonium acetate. The resulting stock solutions were diluted to the desired protein concentrations in 150 mM ammonium acetate (pH 6.8). Protein concentrations were verified by UV-Vis absorption spectroscopy. BLG concentrations throughout this work are expressed on a monomer basis, Hb concentrations are reported on the basis of heterodimeric αβ complexes.

### *Mass Spectrometry*

All mass spectra were recorded under gentle ESI condition using a quadrupole-time-of-flight instrument (Q-TOF Ultima; Waters, Milford, MA, USA). The cone voltage and rf1 lens DC offset were adjusted to provide the highest relative signals for protein noncovalent complexes. Cone voltage values were in the range of 40 to 70 V, and the rf1 voltage was between 50 and 70 V. The desolvation temperature was set to 40 °C, down from its factory-recommended standard value of around 250 °C. The source block temperature was adjusted to 80 °C. Cone and desolvation gas flow rates were 100 and 500 $Lh^{-1}$, respectively. Mass calibration was performed over the range from *m/z* 600 to 7000 using 2 μg $μL^{-1}$ CsI in 1:1 (vol/vol) water/2-propanol. The ion transmission of the quadrupole is strongly dependent on the "MS profile" parameters, as discussed in the Results and Discussion section. Changing the collision cell hexapole rf settings was found to have only minor effects, and all spectra were recorded with a gain of 10 and an offset of 0.8. The maximum signal intensity in the spectra discussed below was on the order of 100 counts per s, roughly one order of magnitude below the saturation level. Increasing the pressure in the source region did not significantly affect the measured $R_{ESI}$ values, revealing that extensive collisional focusing occurs even under standard experimental conditions for the Q-TOF employed here. This is in contrast to other instruments previously used in our laboratory, where the source pressure has dramatic effects [57]. Three different ESI sources were tested, a pulled capillary Waters nanoESI source, an automated chip-based nanoESI system (Advion Triversa, Ithaca, NY, USA), and a regular Waters Z-spray source. The ESI voltages used for the three sources were 1.5–1.8 kV, 1.5–1.7 kV, and 3 kV, respectively. Pulled capillary nanoESI measurements employed borosilicate emitters with a Au/Pd coating (Proxeon, Cambridge, MA, USA). Solution flow for these capillaries was assisted by gentle nitrogen back pressure of less than 1 psi. The nanoESI flow rate under these conditions was estimated gravimetrically to be around 25 nL $min^{-1}$, consistent with the manufacturer's specifications. The nozzles of the Advion nanoESI chips had a diameter of 5 μm, and flow rates were in the range of 50 to 100 nL $min^{-1}$. Flow rates of the Z-spray source were controlled by a syringe pump (Harvard 22, Boston, MA, USA). All spectra were acquired in positive ion mode. Minimum smoothing was applied to the data prior to analysis, using the following MassLynx parameters: *window size*, ±3; *number of smooths*, 2. Peak area measurements for determination of $I_M$ and $I_D$ were conducted by using integration windows of $\Delta m/z = 100$ around each peak.

## Results and Discussion

### *Quadrupole Transmission Profile*

Q-TOF analyzers are the most commonly used type of mass spectrometer for studies on noncovalent protein complexes [16–20]. Intact mass measurements on Q-TOF instruments are conducted by operating the quadrupole ("Q") in rf-only

mode where it serves as an ion guide [58–60]. It is important to note that an rf-only quadrupole does not transmit all ions with the same efficiency. Instead, it acts as a broad-band filter that does not allow passage of species with *m/z* values less than ~0.8 × *M**, where *M** depends on the rf amplitude. On the high mass side the transmission drops gradually, and only ions up to ca. 5 × *M** can pass through the device. Commercial Q-TOF instruments allow the rf amplitude (and hence *M**) to be ramped during data acquisition, thereby permitting analysis of a wider *m/z* window [61].

The choice of rf-only quadrupole settings has dramatic consequences for the relative peak intensities in different *m/z* regions of a mass spectrum. Figure 1 illustrates this effect for Hb. The experiments were conducted under semi-denaturing conditions (pH 3.6), to ensure that the protein exists in various solution phase binding states (unbound α and β subunits, as well as αβ and $(\alpha\beta)_2$ complexes) [56]. Previous studies do not provide sufficient information to predict the concentrations of all these species in solution at pH 3.6. However, the various binding states cover a wide *m/z* range which makes this particular sample well suited for illustrative purposes. For the instrument used here the quadrupole transmission is controlled by seven parameters. $Dwell_1$ and $dwell_2$ reflect the fraction of time that the quadrupole is operated at $M_1^*$ and $M_2^*$, respectively. $Ramp_{12}$ is the time fraction during which the device is ramped from $M_1^*$ to $M_2^*$. Similarly, $ramp_{23}$ refers to the ramp time spent between $M_2^*$ and a third value $M_3^*$. Figure 1 (left hand side panels) depicts transmission profiles that were simulated for different quadrupole parameters, while the panels on the right show the corresponding mass spectra. Except for modifications of these quadrupole parameters, all data in Figure 1 were recorded under identical conditions.

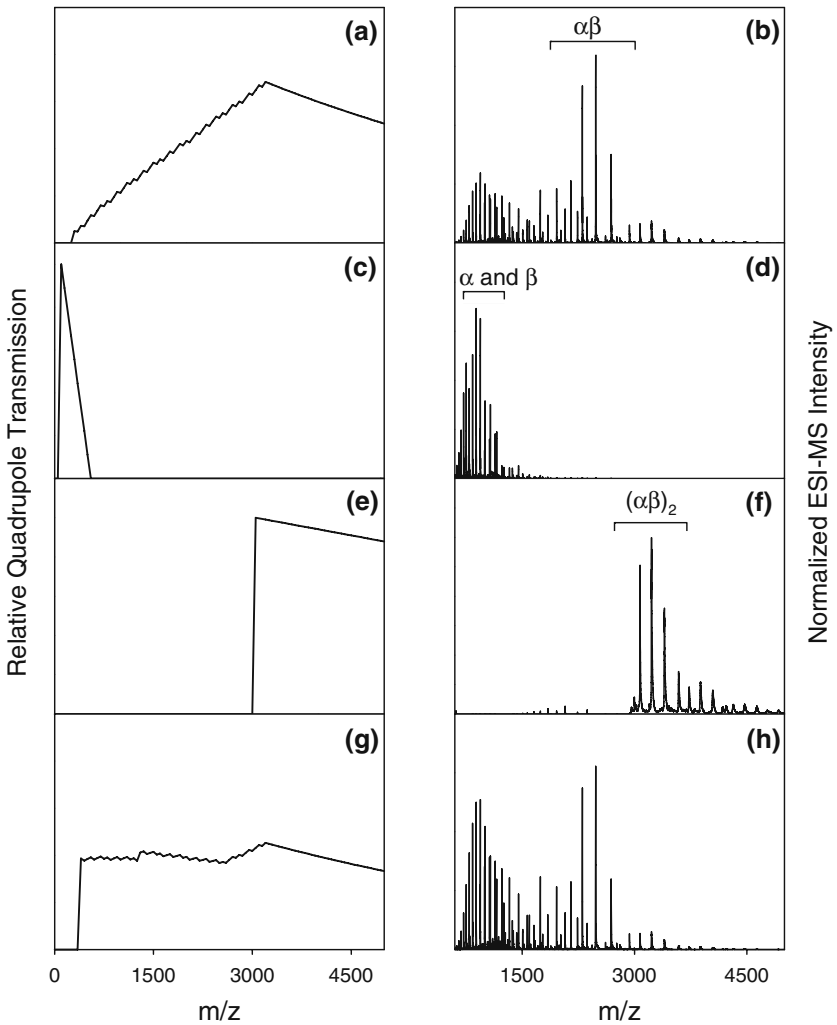


**Figure 1.** Simulated quadrupole transmission profiles (*left*) and corresponding measured ESI mass spectra of Hb (*right*) at pH 3.6. The data were recorded using a Z-spray ESI source with a flow rate of 3 μL $min^{-1}$ and a (αβ) concentration of 100 μM. Parameters for operation of the rf-only quadrupole ($M_1^*$, $dwell_1$, $ramp_{12}$, $M_2^*$, $dwell_2$, $ramp_{23}$, and $M_3^*$) were as follows: (**a**), (**b**) 400, 5%, 95%, 4000, 0%, 0%, 4000; (**c**), (**d**) 100, 100%, 0%, 100, 0%, 0%, 100; (**e**), (**f**) 3800, 100%, 0%, 3800, 0%, 0%, 3800; (**g**), (**h**) 1600, 3%, 0%, 400, 37%, 60%, 4000. Binding states of Hb subunits are indicated as α and β, αβ, and $(\alpha\beta)_2$

When trying to ensure uniform transmission over a wide *m/z* range it is tempting to use settings where the rf amplitude is continuously ramped between a minimum value $M_1$* and a maximum value $M_2$*. Unfortunately, this strategy leads to an overall transmission profile that strongly favors the *m/z* range around $M_2$*, while discriminating against lower values (Figure 1a). This behavior is a consequence of the asymmetric profile shape at any given *M** (see above) [61]. The Hb spectrum recorded under such conditions, with $M_1$*=400 and $M_2$*=4000, is dominated by αβ ions, while peak intensities for $(\alpha\beta)_2$ and unbound subunits are much lower (Figure 1b). Figure 1c, d represent quadrupole settings that were chosen to strongly favor low *m/z* values. The resulting spectrum exclusively shows free α and β species. In contrast, Figure 1e demonstrates the effects of "high mass settings," yielding data that are dominated by $(\alpha\beta)_2$ (Figure 1f). By carefully adjusting the quadrupole rf parameters it is possible to achieve a transmission profile that is relatively uniform between *m/z* 300 and 4500 (Figure 1g). Under these conditions, unbound subunits and αβ appear with comparable peak intensities, while $(\alpha\beta)_2$ signals are much lower (Figure 1h).

Overall, Figure 1 illustrates that ESI mass spectra for samples containing co-existing protein binding states are strongly dependent on the transmission characteristics of the mass analyzer. In fact, the ion intensity ratio of a complex and its unbound constituents can have any value between zero and infinity, depending on the choice of quadrupole settings (Figure 1d, f). It is surprising that the quadrupole transmission properties hardly receive any mention in the pertinent ESI-MS literature, where ion intensity ratios ($R_{ESI\text{-}MS}$, Equation 5) are used to estimate binding affinities in solution. The instrument settings of Figure 1g appear to be most suitable for binding affinity measurements because they result in fairly uniform transmission characteristics. Hence, this profile was used for all subsequent measurements of this work.

## *Effects of Different ESI Sources*

The binding behavior of two model proteins, BLG and Hb was studied by ESI-MS under native solvent conditions (150 mM ammonium acetate, pH 6.8). BLG forms homodimers in solution. X-ray analyses of the binding interface show a number of hydrogen bonds between the AB loops of both subunits. Inter-subunit H-bonds also occur between two β strands, in addition to a pair of salt bridges [32, 52, 53]. Hb is usually referred to as a "dimer of dimers," because its solution phase behavior is dominated by $(\alpha\beta)_2$ = 2 αβ equilibration under native conditions [54–56, 62]. Subunit interactions in Hb are mediated by nonpolar and van der Waals contacts, as well as hydrogen bonds and salt bridges [63]. Hb dissociation into unbound α and β only plays a role under non-native conditions, as in Figure 1 [54–56]. On the basis of these considerations, the dissociation behavior of both BLG and Hb can be interpreted within the framework provided by Equations 1–9. For Hb, this requires αβ and $(\alpha\beta)_2$ to be interpreted as "*M*" and "*D*," respectively.

Mass spectra of both protein systems were acquired under four different ionization conditions: (1) nanoESI employing a pulled capillary emitter, (2) an automated chip-based nanoESI source, and a regular Z-spray ESI source operated at (3) 1 μL $min^{-1}$ and (4) 50 μL $min^{-1}$. Data acquired for BLG show monomers and homodimers, consistent with earlier observations (Figure 2) [32, 52]. Analysis of these spectra reveals that the apparent extent of BLG dimerization under all four ionization conditions is quite similar, with $f_{ESI\text{-}MS}$ values of 0.69, 0.66, 0.79, and 0.72 for Figure 2a, c, e, and g, respectively. Similar measurements were conducted with Hb, for assessing the abundance of αβ and $(\alpha\beta)_2$ ions. Native Hb mass spectra obtained under the four ionization conditions resulted in $f_{ESI\text{-}MS}$ values of 0.70, 0.67, 0.83, and 0.80 (Figure 2b, d, f, h, respectively). As expected [54–56], unbound

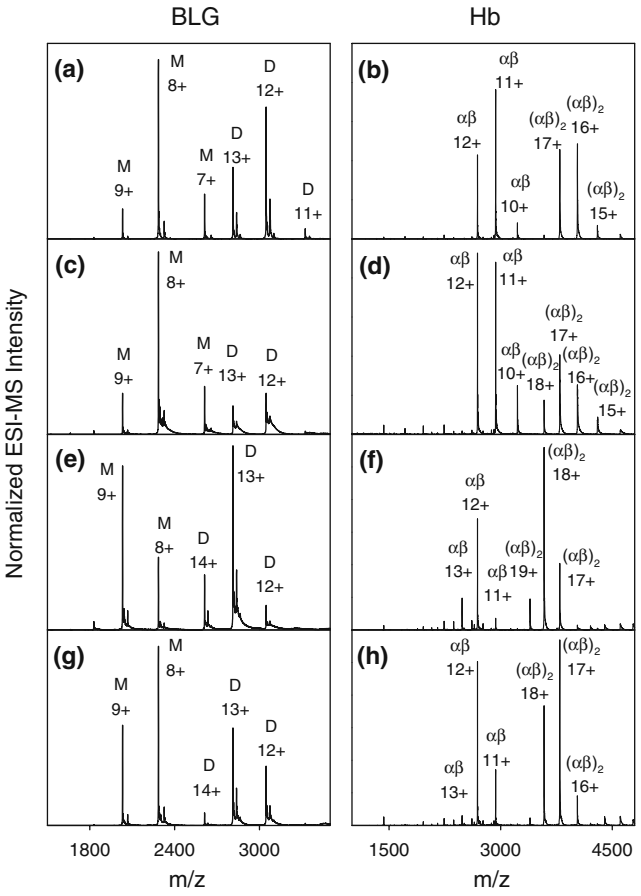


**Figure 2.** ESI mass spectra of 10 μM BLG (*panels on left*), and 34 μM Hb (*panels on right*). The data were acquired with a (**a**), (**b**) pulled capillary nanoESI source, (**c**), (**d**) chip-based nanoESI source, (**e**), (**f**) Z-spray ESI source at 1 μL $min^{-1}$, and (**g**), (**h**) Z-spray ESI source at 50 μL $min^{-1}$. *M* and *D* in the BLG spectra denote monomers and dimers, respectively. Binding states of Hb subunits are denoted as αβ and $(\alpha\beta)_2$, with protonation states indicated. Except for differences in ESI voltage (see text), all spectra were acquired using identical instrument settings

α and β are virtually undetectable for the solvent conditions of Figure 2.

The data of Figure 2 demonstrate that the choice of ion source can affect the outcome of binding affinity measurements to a certain extent. However, the differences are surprisingly small, as $f_{ESI\text{-}MS}$ values measured under the four conditions agree within 25%. Our observations do *not* support the commonly held notion that nanoESI is "softer" and, thus, better suited for studying noncovalent systems, at least not for the proteins studied here. This finding is in line with the results of other protein binding experiments [26, 46]. Consistent with earlier reports [17, 47], we also found nanoESI-MS signals to be not as stable, and the resulting spectra to be less reproducible than those acquired with a regular ESI source. This effect may be caused by clogging of the very narrow nanoESI sprayer apertures. If $f_{ESI\text{-}MS}$ values are to be used for judging the quality of the spectra in Figure 2, one has to conclude that a regular ESI source operated at 1 μL $min^{-1}$ provides the most favorable conditions for the observation of protein complexes (Figure 2e, f).

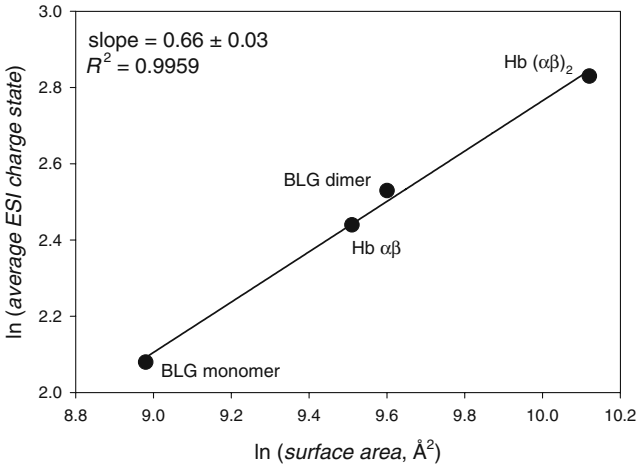


**Figure 3.** Plot of ln(average ESI charge state) versus ln (surface area, Å$^2$), following the approach of ref [65]. Average charge states for each protein were calculated as described previously [38] on the basis of integrated peak areas, averaged over all spectra shown in Figure 2. Solvent accessible surface areas were calculated for BLG monomers and dimers from pdb file 1BEB using the program GetArea (http://curie.utmb.edu/getarea.html). PDB file 2QSS for used for Hb

## *Testing the Fidelity of ESI-MS Data for Affinity Measurements*

Several potential pitfalls have to be considered when assessing the solution-phase binding affinity of protein complexes by ESI-MS (see Section 1). Luckily, the most pertinent points are addressable by direct analysis of the measured spectra.

Protein binding in solution can be associated with conformational changes. In these cases the subunits will be more tightly folded within the complex than in the free state [64]. Such a scenario should increase the response factor $\gamma_M$ relative to $\gamma_D$ (Equation 6) because partial unfolding enhances the effective hydrophobicity and thereby increases the ionization efficiency [38, 40]. Whether or not this case applies to the systems studied here can be determined by applying a simple test. The average ESI charge state is linked to the protein surface area in solution. For natively folded proteins a linear relationship between ln(surface area) and ln(average ESI charge state) has been demonstrated, with a slope of 0.69 ± 0.02 [65]. Figure 3 shows a ln–ln plot of this type for BLG monomers and dimers, as well as for Hb αβ and $(\alpha\beta)_2$. All data points fall on a straight line with a slope of 0.66±0.03, consistent with the results of Kaltashov and Mohimen [65]. Solution-phase unfolding greatly enhances the degree of protonation during ESI [66–69], and therefore would lead to major deviations from linear behavior in Figure 3. Thus, we conclude that complex formation is not associated with major conformational changes for the proteins studied here. In other words, a selective enhancement of free protein signals ($\gamma_M$) caused by conformational effects can be excluded.

Another point that has to be addressed is the possible disruption of noncovalent complexes by CID during ion sampling or transport [27, 49]. In other words, we have to scrutinize whether BLG monomer peaks and Hb αβ signals in Figure 2 encompass significant contributions from inadvertently formed gas phase fragments. Charge partitioning during CID can occur in a symmetric or asymmetric fashion, subject to conservation of overall charge [70]. On the basis of the very narrow charge state distributions for both BLG monomers and Hb αβ ions (Figure 2), CID with asymmetric charge partitioning can immediately be excluded. On the other hand, symmetric fragmentation of BLG dimers would result in monomeric species with charge states centered around 13/2 ≈ 6–7, whereas $(\alpha\beta)_2$ would produce αβ fragments with charges in the range of 17/2 ≈ 8–9. The observed charge states for both BLG monomers and Hb αβ ions fall outside these expected ranges (Figure 2). This behavior implies that the extent of inadvertent gas phase fragmentation is negligible for the conditions used here. In the case of Hb, this conclusion is further supported by earlier experiments where CID of $(\alpha\beta)_2$ was deliberately induced, resulting in spectra that are completely different from those depicted in Figure 2 [58].

A third potential concern is the formation of nonspecific protein–protein complexes during ESI [32, 35, 45]. Such an effect would lead to an overrepresentation of bound protein states in the spectra. Any ESI-mediated clustering should be strongly dependent on the size of the initially formed ESI droplets. The volume of these droplets is proportional to the solution flow rate [38, 71–73]. Larger droplets undergo a greater number of evaporation/fission cycles, thereby increasing the protein concentration in the final droplets that produce gas phase analyte ions [17, 35]. Thus, the formation

of nonspecific aggregates should be enhanced at higher flow rates, thereby providing a tool for assessing whether or not clustering artifacts occur under the experimental conditions used. Comparison of mass spectra recorded at 1 μL $min^{-1}$ (Figure 2e, f) and 50 μL $min^{-1}$ (Figure 2g, h) show that increasing the flow rate does *not* lead to higher signals for bound species. Therefore, the $f_{ESI\text{-}MS}$ values measured for BLG and Hb are not significantly affected by nonspecific clustering. It is interesting to note that abundance of dimeric BLG and Hb $(\alpha\beta)_2$ actually *de*creases slightly when the flow rate is raised. This may be due to more favorable desolvation at 1 μL $min^{-1}$ (Figure 2e, f).

In summary, the spectra of Figure 2 appear to be free of major ESI-induced complexation and fragmentation artifacts. Moreover, the linear relationship of Figure 3 suggests that conformationally-induced differences in the ionization efficiency of free and bound proteins are small. The quadrupole transmission has been adjusted to ensure that *m/z*-dependent discrimination effects are at a minimum (Figure 1g). Only after considering all of these points, it is justified to assume that $\gamma_M \approx \gamma_D$ (Equation 6). Hence, the value of $R_{ESI\text{-}MS}$ should closely match the concentration ratio $R_{sol}$ (Equation 7), such that dissociation constants can be determined directly from ESI-MS intensity ratios (Equation 4). The validity of these considerations is confirmed by the results discussed in the subsequent section.

### *Concentration-Dependent Measurements*

For any dissociation equilibrium in solution (Equation 1), the fraction of bound protein depends on the total concentration $[P]_0$. Elevated protein concentrations will increase the value of $f_{sol}$. Figure 4 depicts the results of comparative ESI measurements on BLG and Hb, where $[P]_0$ was altered by two orders of magnitude. The data were acquired using a standard Z-spray ESI source at 1 μL $min^{-1}$. As expected, the resulting spectra show an increased abundance of bound protein at elevated $[P]_0$. Dissociation constants were determined from the measured $R_{ESI}$ values at different $[P]_0$, assuming that $\gamma_M/\gamma_D = 1$ (Equations 4, 7). The resulting $K_d$ values are summarized in Table 1. BLG dissociation constants determined in this way at different protein concentrations agree within a factor of two. When averaging these data a value of $K_d = (2.2 \pm 0.7)$ μM is obtained. This result is in reasonable agreement with the literature value of 4.9 μM, which was measured by AUC for BLG [53]. The spread in the ESI-MS-derived $K_d$ values for Hb is somewhat larger, between 1.3 and 3.6 μM. However, this level of variability is quite common when measuring dissociation constants under different conditions [74]. Most importantly, the average $K_d$ value of (2.4±1) μM for Hb is consistent with a the results of various solution-phase assays that provided a dissociation constant of 2 μM [62, 75].

The fact that similar $K_d$ values are obtained at different protein concentrations confirms that the spectral changes seen in Figure 4 indeed reflect equilibrium shifts in solution. More importantly, the consistency of ESI-MS-derived $K_d$ values with previous solution-phase data provides an *a posteriori* justification for the supposition that $\gamma_M \approx \gamma_D$ under the carefully adjusted conditions of this work.

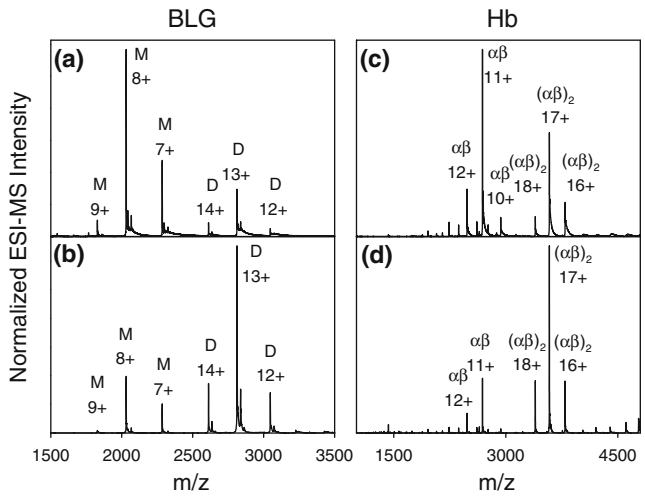


**Figure 4.** ESI mass spectra of BLG acquired at a protein concentration of (**a**) 1 μM [$f_{ESI-MS}$=0.36] and (**b**) 90 μM [$f_{ESI-MS}$=0.89]. Panels (**c**), (**d**) show data measured for 3.4 μM and 170 μM Hb, with $f_{ESI-MS}$ values of 0.65 and 0.90, respectively. The data were recorded using a Z-spray ESI source at 1 μL $min^{-1}$

## Conclusions

This work demonstrates the feasibility of using the direct ESI-MS approach for quantitative measurements of protein–protein binding affinities ($K_d$ values) in solution. Special care must be taken to ensure that the data obtained in these experiments are not affected by artifacts related to the ionization or detection processes. In contrast to protein–small molecule complexes, free and bound forms of protein–protein assemblies cover a much wider *m/z* range in the spectra. This aspect leads to unique challenges. A key aspect that has received little attention in previous studies is the parameter setting of rf-only quadrupoles in the ion path. Only carefully adjusted conditions provide a relatively uniform transmission profile. When studying protein–protein assemblies, practitioners may by tempted to employ quadrupole parameters that maximize the relative abundance of bound species. It can be very misleading to employ data acquired under such skewed conditions for affinity measure-

**Table 1.** Dissociation constants $K_d$ measured by ESI-MS at different protein concentrations $[P]_0$. The data used for these calculations were acquired using a regular Z-spray ESI source operated at 1 μL $min^{-1}$ (Figures 2, 4). All values are in units of μM

| | | | | |
|---|---|---|---|---|
| BLG | $[P]_0$ | 1 | 10 | 90 |
| | $K_d$ | 2.2 | 1.2 | 2.5 |
| Hb | $[P]_0$ | 3.4 | 34 | 170 |
| | $K_d$ | 1.3 | 2.4 | 3.6 |

ments (Figure 1). In addition, we caution that other ion optics such as hexapoles and stacked lenses may also be associated with *m/z*-dependent discrimination effects [58]. Some of these factors are not easily controllable by the user, and they are not as well characterized as the quadrupole behavior. A proper test for the uniformity of the overall transmission profile is the comparison between ESI-MS-derived $K_d$ values and solution-phase measurements for a number of well studied model systems.

Except for its lower sample consumption, the use of nanoESI does not offer any advantages for the two protein systems studied in this work. In fact, the highest abundance of BLG dimers and Hb $(\alpha\beta)_2$ complexes (and the best agreement with previously measured $K_d$ values) was obtained with a regular ESI source operated at 1 μL $min^{-1}$ (Figure 2).

Spectra of protein–protein complexes and their free constituents can be subjected to a number of simple controls. In cases where formation of a protein complex is associated with major conformational changes the ionization efficiencies of free and bound forms are expected to be significantly different. For complexes with known X-ray structures, a ln–ln plot of the type depicted in Figure 3 is a useful tool for determining whether or not such conformational factors occur. Comparison of the ESI charge states for free and bound species gives an indication whether the measured spectra are affected by CID artifacts. Flow-rate-dependent measurements can reveal the extent to which nonspecific aggregates are formed. Another test for the fidelity of the direct ESI-MS approach is binding affinity measurement conducted at various protein concentrations, all of which should provide very similar values of $K_d$. In future work it will be interesting to extend the measurements of this study to a range of other protein complexes. We are hopeful that the direct ESI-MS approach will become well-established for determining protein–protein binding affinities, similar to the case of protein–small molecule interactions where this strategy is already fairly commonplace.

## Acknowledgments

The authors acknowledge support for this study by the Natural Sciences and Engineering Research Council of Canada (NSERC), the Canada Foundation for Innovation (CFI), the Province of Ontario, the Canada Research Chairs Program, and The University of Western Ontario. Lee-Ann Briere and Stanley D. Dunn are acknowledged for their help during the initial stages of this work. The authors also thank Paula Pittock and Gilles Lajoie for the loan of a nanoESI source.

## References

1. Robinson, C.V., Sali, A., Baumeister, W.: The molecular sociology of the cell. *Nature* **450**, 973–982 (2007)
2. van Holde, K., Johnson, W., Shing Ho, P.: Principles of physical biochemistry, 2nd edn. Pearson Prentice Hall, Upper Saddle River, NJ (2006)
3. Hajduk, P., Meadows, R.P., Fesik, S.W.: NMR-based screening in drug discovery. *Q. Rev. Biophys.* **32**, 211–240 (1999)
4. McDonnell, J.M.: Surface plasmon resonance: towards an understanding of the mechanisms of biological molecular recognition. *Curr. Opin. Chem. Biol.* **5**, 572–577 (2001)
5. Zhu, H., Bilgin, M., Bangham, R., Hall, D., Casamayor, A., Bertone, P., Lan, N., Jansen, R., Bidlingmaier, S., Houfek, T., Mitchell, T., Miller, P., Dean, R.A., Gerstein, M., Snyder, M.: Global analysis of protein activities using proteome chips. *Science* **293**, 2101 (2001)
6. Titz, B., Schlesner, M., Uetz, P.: What do we learn from high-throughput protein interaction data? *Exp. Rev. Proteom.* **1**, 111–121 (2004)
7. Cole, J.L., Hansen, J.C.: Analytical ultracentrifugation as a contemporary biomolecular research tool. *J. Biomol. Tech.* **10**, 163–176 (1999)
8. Clark, S.M., Konermann, L.: Determination of ligand–protein dissociation constants by electrospray mass spectrometry-based diffusion measurements. *Anal. Chem.* **76**, 7077–7083 (2004)
9. Xu, Y., Schmitt, S., Tang, L., Jakob, U., Fitzgerald, M.C.: Thermodynamic analysis of a molecular chaperone binding to unfolded protein substrates. *Biochemistry* **49**, 1346–1353 (2010)
10. Zhu, M.M., Rempel, D.L., Du, Z., Gross, M.L.: Quantification of protein–ligand interactions by mass spectrometry, titration, and H/D exchange: PLIMSTEX. *J. Am. Chem. Soc.* **125**, 5252–5253 (2003)
11. Marcsisin, S.R., Engen, J.R.: Hydrogen exchange mass spectrometry: what is it and what can it tell us? *Anal. Bioanal. Chem.* **397**, 967–972 (2010)
12. Xu, G., Chance, M.R.: Hydroxyl radical-mediated modification of proteins as probes for structural proteomics. *Chem. Rev.* **107**, 3514–3543 (2007)
13. Mendoza, V.L., Vachet, R.W.: Probing protein structure by amino acid-specific covalent labeling and mass spectrometry. *Mass Spectrom. Rev.* **28**, 785–815 (2009)
14. Rigaut, G., Shevchenko, A., Rutz, B., Wilm, M., Mann, M., Seraphin, B.: A generic protein purification method for protein complex characterization and proteome exploration. *Nat. Biotechnol.* **17**, 1030–1032 (1999)
15. Schriemer, D.C.: Biosensor alternative: frontal affinity chromatography. *Anal. Chem.* **76**, 441A–448A (2004)
16. Loo, J.A.: Studying noncovalent protein complexes by electrospray ionization mass spectrometry. *Mass Spectrom. Rev.* **16**, 1–23 (1997)
17. Benesch, J.L.P., Ruotolo, B.T., Simmons, D.A., Robinson, C.V.: Protein complexes in the gas phase: technology for structural genomics and proteomics. *Chem. Rev.* **107**, 3544–3567 (2007)
18. Heck, A.J.R., Van den Heuvel, R.H.H.: Investigation of intact protein complexes by mass spectrometry. *Mass Spectrom. Rev.* **23**, 368–389 (2004)
19. Daniel, J.M., Friess, S.D., Rajagopalan, S., Wendt, S., Zenobi, R.: Quantitative determination of noncovalent binding interactions using soft ionization mass spectrometry. *Int. J. Mass Spectrom.* **216**, 1–27 (2002)
20. Ashcroft, A.E.: Mass spectrometry and the amyloid problem—How far can we go in the gas phase? *J. Am. Soc. Mass Spectrom.* **21**, 1087–1096 (2010)
21. Ganem, B., Li, Y.-T., Henion, J.D.: Observation of noncovalent enzyme–substrate and enzyme–product complexes by ion-spray mass spectrometry. *J. Am. Chem. Soc.* **113**, 7818–7819 (1991)
22. Katta, V., Chait, B.T.: Observation of the heme–globin complex in native myoglobin by electrospray-ionization mass spectrometry. *J. Am. Chem. Soc.* **113**, 8534–8535 (1991)
23. Frycak, P., Schug, K.A.: On-line dynamic titration: determination of dissociation constants for noncovalent complexes using gaussian concentration profiles by electrospray ionization mass spectrometry. *Anal. Chem.* **79**, 5407–5413 (2007)
24. Rostom, A.A., Fucini, P., Benjamin, D.R., Juenemann, R., Nierhaus, K. H., Hartl, F.U., Dobson, C.M., Robinson, C.V.: Detection and selective dissociation of intact ribosomes in a mass spectrometer. *Proc. Natl. Acad. Sci. U.S.A.* **97**, 5185–5190 (2000)
25. Bothner, B., Siuzdak, G.: Electrospray ionization of a whole virus: analyzing mass, structure, and viability. *Chem. Bio. Chem.* **5**, 258–260 (2004)
26. Jecklin, M.C., Touboul, D., Bovet, C., Wortmann, A., Zenobi, R.: Which electrospray-based ionization method best reflects protein–ligand interactions found in solution? A comparison of ESI, nanoESI, and ESSI for the determination of dissociation constants

with mass spectrometry. *J. Am. Soc. Mass Spectrom.* **19**, 332–343 (2008)
27. Wang, W., Kitova, E.N., Klassen, J.S.: Influence of solution and gas phase processes on protein–carbohydrate binding affinities determined by nanoelectrospray fourier transform ion cyclotron resonance mass spectrometry. *Anal. Chem.* **75**, 4945–4955 (2003)
28. Jørgensen, T.J.D., Roepstorff, P., Heck, A.J.R.: Direct determination of solution binding constants for noncovalent complexes between bacterial cell wall peptide analogues and vancomycin group antibiotics by electrospray ionization mass spectrometry. *Anal. Chem.* **70**, 4427–4432 (1998)
29. Pan, J., Xu, K., Yang, X., Choy, W.Y., Konermann, L.: Solution-phase chelators for suppressing nonspecific protein–metal interactions in electrospray mass spectrometry. *Anal. Chem.* **81**, 5008–5015 (2009)
30. Gabelica, V., Rosu, F., De Pauw, E.: A simple method to determine electrospray response factors of noncovalent complexes. *Anal. Chem.* **81**, 6708–6715 (2009)
31. Wilcox, J.M., Rempel, D.L., Gross, M.L.: Method of measuring oligonucleotide-metal affinities: interactions of the thrombin binding aptamer with K + and Sr2+. *Anal. Chem.* **80**, 2365–2371 (2008)
32. Sun, J., Kitova, E.N., Sun, N., Klassen, J.S.: Method for identifying nonspecific protein–protein interactions in nanoelectrospray ionization mass spectrometry. *Anal. Chem.* **79**, 8301–8311 (2007)
33. Chalcraft, K.R., Lee, R.C.M., Britz-McKibbin, P.: Virtual quantification of metabolites by capillary electrophoresis-electrospray ionization-mass spectrometry: predicting ionization efficiency without chemical standards. *Anal. Chem.* **81**, 2506–2515 (2009)
34. Oss, M., Kruve, A., Herodes, K., Leito, I.: Electrospray ionization efficiency scale of organic compounds. *Anal. Chem.* **82**, 2865–2872 (2010)
35. Peschke, M., Verkerk, U.H., Kebarle, P.: Features of the ESI mechanism that affect the observation of multiply charged noncovalent protein complexes and the determination of the association constant by the titration method. *J. Am. Soc. Mass Spectrom.* **15**, 1424–1434 (2004)
36. Chernushevich, I.V., Thomson, B.A.: Collisional cooling of large ions in electrospray mass spectrometry. *Anal. Chem.* **76**, 1754–1760 (2004)
37. Schmidt, A., Bahr, U.M.K.: Influence of pressure in the first pumping stage on analyte desolvation and fragmentation in Nano-ESI MS. *Anal. Chem.* **73**, 6040–6046 (2001)
38. Kuprowski, M.C., Konermann, L.: Signal response of co-existing protein conformers in electrospray mass spectrometry. *Anal. Chem.* **79**, 2499–2506 (2007)
39. Null, A.P., Nepomuceno, A.I., Muddiman, D.C.: Implications of hydrophobicity and free energy of solvation for characterization of nucleic acids by electrospray ionization mass spectrometry. *Anal. Chem.* **75**, 1331–1339 (2003)
40. Cech, N.B., Enke, C.G.: Practical implication of some recent studies in electrospray ionization fundamentals. *Mass Spectrom. Rev.* **20**, 362–387 (2001)
41. Van Berkel, G.J., Zhou, F., Aronson, J.T.: Changes in bulk solution pH caused by the inherent controlled-current electrolytic process of an electrospray ion source. *Int. J. Mass Spectrom. Ion Process.* **162**, 55–67 (1997)
42. Konermann, L., Silva, E.A., Sogbein, O.F.: Electrochemically induced pH changes resulting in protein unfolding in the ion source of an electrospray mass spectrometer. *Anal. Chem.* **73**, 4836–4844 (2001)
43. Wang, H., Agnes, G.R.: Kinetically labile equilibrium shifts induced by the electrospray process. *Anal. Chem.* **71**, 4166–4172 (1999)
44. Wortmann, A., Kistler-Momotova, A., Zenobi, R., Heine, M.C., Wilhelm, O., Pratsinis, S.E.: Shrinking droplets in electrospray ionization and their influence on chemical equilibria. *J. Am. Soc. Mass Spectrom.* **18**, 385–393 (2007)
45. Hossain, B.M., Konermann, L.: Pulsed hydrogen/deuterium exchange MS/MS for studying the relationship between noncovalent protein complexes in solution and in the gas phase after electrospray ionization. *Anal. Chem.* **78**, 1613–1619 (2006)
46. Loo, J.A.: Electrospray ionization mass spectrometry: a technology for studying noncovalent macromolecular complexes. *Int. J. Mass Spectrom.* **200**, 175–186 (2000)
47. Bovet, C., Wortmann, A., Eiler, S., Granger, F., Ruff, M., Gerrits, B., Moras, D., Zenobi, R.: Estrogen receptor–ligand complexes measured by chip-based nanoelectrospray mass spectrometry: an approach for the screening of endocrine disruptors. *Protein Sci.* **16**, 938–946 (2007)
48. Bich, C., Baer, S., Jecklin, M.C., Zenobi, R.: Probing the hydrophobic effect of noncovalent complexes by mass spectrometry. *J. Am. Soc. Mass Spectrom.* **21**, 286–289 (2010)
49. Tesic, M., Wicki, J., Poon, D.K.Y., Withers, S.G., Douglas, D.J.: Gas phase noncovalent protein complexes that retain solution binding properties: binding of xylobiose inhibitors to the b-1, 4 exoglucanase from *Cellulomonas fimi*. *J. Am. Soc. Mass Spectrom.* **18**, 64–73 (2007)
50. Wilm, M., Mann, M.: Analytical properties of the nanoelectrospray ion source. *Anal. Chem.* **68**, 1–8 (1996)
51. Juraschek, R., Dulcks, T., Karas, M.: Nanoelectrospray—more than just a minimized-flow electrospray ionization source. *J. Am. Soc. Mass Spectrom.* **10**, 300–308 (1999)
52. Invernizzi, G., Samalikova, M., Brocca, S., Lotti, M., Molinari, H., Grandori, R.: Comparison of bovine and porcine b-Lactoglobulin: a mass spectrometric analysis. *J. Mass Spectrom.* **41**, 717–727 (2006)
53. Sakurai, K., Goto, Y.: Manipulating monomer-dimer equilibrium of bovine b-Lactoglobulin by amino acid substitution. *J. Biol. Chem.* **277**, 25735–25740 (2002)
54. Eaton, W.A., Henry, E.R., Hofrichter, J., Mozzarelli, A.: Is cooperative oxygen binding by hemoglobin really understood. *Nat. Struct. Biol.* **6**, 351–358 (1999)
55. Perutz, M.F.: Stereochemistry of cooperative effects in hemoglobin. *Nature* **228**, 726–739 (1970)
56. Boys, B.L., Kuprowski, M.C., Konermann, L.: Symmetric behavior of hemoglobin a- and b-Subunits during acid-induced denaturation observed by electrospray mass spectrometry. *Biochemistry* **46**, 10675–10684 (2007)
57. Boys, B.L., Konermann, L.: Folding and assembly of hemoglobin monitored by electrospray mass spectrometry using an on-line dialysis system. *J. Am. Soc. Mass Spectrom.* **18**, 8–16 (2007)
58. Chernushevich, I.V., Loboda, A.V., Thomson, B.A.: An introduction to quadrupole time-of-flight mass spectrometry. *J. Mass Spectrom.* **36**, 849–865 (2001)
59. Douglas, D.J.: Linear quadrupoles in mass spectrometry. *Mass Spectrom. Rev.* **28**, 937–960 (2009)
60. March, R., Todd, J.F.J.: Quadrupole ion trap mass spectrometry, 2nd edn. Wiley, New York; Toronto (2005)
61. Sobott, F., Hernandez, H., McCammon, M.G., Tito, M.A., Robinson, C. V.: A tandem mass spectrometer for improved transmission and analysis of large macromolecular assemblies. *Anal. Chem.* **74**, 1402–1407 (2002)
62. Thomas, J.O., Edelstein, S.J.: Observation of the dissociation of unliganded hemoglobin. *J. Biol. Chem.* **247**, 7870–7874 (1972)
63. Antonini, E., Brunori, M.: Hemoglobin and myoglobin in their reactions with ligands, vol. xxi. North-Holland Publishing Company, Amsterdam, London (1971)
64. Gunasekaran, K., Tsai, C.-J., Kumar, S., Zanuy, D., Nussinov, R.: Extended disordered proteins: targeting function with less scaffold. *Trends Biochem. Sci.* **28**, 81–85 (2003)
65. Kaltashov, I.A., Mohimen, A.: Estimates of protein surface area in solution by electrospray ionization mass spectrometry. *Anal. Chem.* **77**, 5370–5379 (2005)
66. Dobo, A., Kaltashov, I.A.: Detection of multiple protein conformational ensembles in solution via deconvolution of charge-state distributions in ESI MS. *Anal. Chem.* **73**, 4763–4773 (2001)
67. Grandori, R.: Detecting equilibrium cytochrome *c* folding intermediates by electrospray ionization mass spectrometry: two partially folded forms populate the molten globule state. *Protein Sci.* **11**, 453–458 (2002)
68. Konermann, L., Douglas, D.J.: Acid-induced unfolding of cytochrome *c* at different methanol concentrations: electrospray ionization mass spectrometry specifically monitors changes in the tertiary structure. *Biochemistry* **36**, 12296–12302 (1997)
69. Borysic, A.J.H., Radford, S.E., Ashcroft, A.E.: Co-populated conformational ensembles of b2-microglobulin uncovered quantitatively by electrospray ionization mass spectrometry. *J. Biol. Chem.* **279**, 27069–27077 (2004)
70. Jurchen, J.C., Williams, E.R.: Origin of asymmetric charge partitioning in the dissociation of gas-phase protein homodimers. *J. Am. Chem. Soc.* **125**, 2817–2826 (2003)
71. Pan, P., McLuckey, S.A.: Electrospray ionization of protein mixtures at low pH. *Anal. Chem.* **75**, 1491–1499 (2003)

72. Loscertales, I.G., de la Mora, J.F.: Experiments on the kinetics of field evaporation of small ions from droplets. *J. Chem. Phys.* **103**, 5041–5060 (1995)
73. Schmidt, A., Karas, M., Dülcks, T.: Effect of different solution flow rates on analyte signals in Nano-ESI MS, or: when does ESI turn into Nano-ESI. *J. Am. Soc. Mass Spectrom.* **14**, 492–500 (2003)
74. Powell, K.D., Ghaemmaghami, S., Wang, M.Z., Ma, L., Oas, T.G., Fitzgerald, M.C.: A general mass spectrometry-based assay for the quantitation of protein–ligand binding interactions in solution. *J. Am. Chem. Soc.* **124**, 10256–10257 (2002)
75. Riggs, A.F.: Self-association, cooperativity, and supercooperativity of oxygen binding by hemoglobins. *J. Exper. Biol.* **201**, 1073–1084 (1998)